

## Research Paper

# Active Vibration Control with Multi-Objective Control Output for Typical Engineering Equipment

Xu JIAN<sup>1)</sup>, Zhang TONG-YI<sup>2)</sup>, Huang WEI<sup>2)</sup>, Hu MING-YI<sup>2)</sup>

<sup>1)</sup> *China National Machinery Industry Corporation*  
Danning Street 3, Haidian District, Beijing, P. R. China

<sup>2)</sup> *China IPPR International Engineering Co., Ltd*  
West 3rd Ring North Road 5, Haidian District, Beijing, P.R. China  
e-mail: huangweiac@126.com, huangwei@ippr.net

In traditional active vibration control, a single-objective control output is often considered and constrained, but in fact some conflicting performance indexes are always emerging simultaneously and a one-sided method for pursuing only one excellent output is adopted, which may sacrifice other control characteristics. In this paper, a novel active vibration control with multi-objective control output was proposed for machinery equipment and sensitive equipment, and the latest artificial intelligence – multi-objective particle swarm optimization (MOPSO) was utilized, and the active controller was evaluated by the  $H_\infty$  criterion, meanwhile an active control with a single-objective control output was also carried out for comparison. Numerical studies demonstrated that a pair of conflicting indexes could be balanced well in the proposed strategy, and thus only one blindly pursued control output was effectively overcome.

**Key words:** MOPSO, active vibration control, multi-objective control output, equipment.

## 1. INTRODUCTION

The rapid development of modern industry is closely related to broad application and innovation of engineering equipment. Such equipment can be classified into two major types, one including rotating, reciprocating, impacting and other machinery equipment, and the other mainly including vibration sensitive equipment, high-precision grinding equipment, measuring equipment, etc. Vibration control is necessary for the mentioned equipment and reducing the vibration of machinery equipment can effectively reduce the severe force transmitted to the surrounding environment, and a similar measure is also essential for keeping the sensitive equipment away from surrounding environmental vibration.

The passive method is the most basic approach that does not require any external energy, and it is also the simplest method to perform vibration isola-

tion [1]. However, passive design is difficult to be implemented for low frequency vibration and often requires a compromise between isolation performance and equipment alignment [2]. To overcome these shortcomings, active control strategies [3–7] have recently emerged in the research such as PID [8],  $H_\infty$  [9], and fuzzy logic [10] method. Control output is merely single objective in traditional active controls or in other words vibration suppression only meets one established index, but the other accompanying indexes are ignored. A comprehensive consideration for multi-objective control output for active vibration control is rare in recent studies, for example the vibrating level of machinery equipment should be controlled effectively when the force transmitted from equipment to foundation is reduced, which is closely related to the machinery life, durability and safety. Similarly, the deformation of vibration isolators directly affects the performance accuracy of the sensitive equipment and it is therefore inadequate in controlling the vibration of equipment.

The conventional optimization methods using derivatives and gradients are generally not able to locate or identify the global optimum. Recently, heuristic methods have been widely used for the global optimization. Particle swarm optimization (PSO) was first proposed by EBERHART and KENNEDY [11], and it is a novel population-based metaheuristic optimization method. Since then using the swarm intelligence generated by the cooperation and competition between the particles in a swarm has become a useful tool for engineering optimization. FARSHIDIANFAR *et al.* [12] used the PSO technique to design a  $H_\infty$  controller for machinery and sensitive equipment, and their numerical results showed that feedback controller using the PSO algorithm and  $H_\infty$  criterion could obtain perfect performance to reduce the harmful vibrations and disturbances. COELLO *et al.* [13] first proposed the multi-objective particle swarm optimization (MOPSO), in which the *Pareto* sets and non-dominated solutions were the core strategies.

## 2. BRIEF INTRODUCTIONS TO PSO AND MOPSO

The PSO algorithm is a random optimization method based on swarm intelligence. This algorithm is inspired by the social behavior and the organisms' movement in a bird flock, and it employs a swarm of multiple particles, each with their own position and velocity. All particles share information obtained from other particles, and interaction among the particles makes the search efficient. Each potential solution is also assigned a randomized velocity and potential solutions are called particles. These particles are then “flown” through hyperspace. Each particle keeps track of its own coordinates in the hyperspace, which are associated with the best solution (fitness) it has achieved so far. This solution is referred to as ‘*pbest*’. All values of *pbest* for each of the particles are tracked

simultaneously. By keeping track of the overall best value, and its location, the globally optimized solution-*gbest* can be obtained [14].

Updating the velocities and positions of each particle are core parts of the PSO algorithm and are described as

$$(2.1) \quad \mathbf{v}_{ij}(t+1) = \omega \mathbf{v}_{ij}(t) + c_1 r_1 (pbest_{ij}(t) - \mathbf{x}_{ij}(t)) + c_2 r_2 (gbest_{ij}(t) - \mathbf{x}_{ij}(t)),$$

$$(2.2) \quad \mathbf{x}_{ij}(t+1) = \mathbf{x}_{ij}(t) + \mathbf{v}_{ij}(t+1),$$

where  $i$  represents the  $i$ -th particle,  $j$  represents the  $j$ -th dimension of each particle,  $v_{ij}(t)$  is the flight velocity component of  $j$ -th dimension of particles,  $x_{ij}(t)$  is the flight displacement component of the  $j$ -th dimension in the  $t$ -th generation,  $pbest$  represents the local optimum,  $gbest$  represents the global optimum,  $c_1$ ,  $c_2$  are learning factors,  $r_1$ ,  $r_2$  are random numbers between (0, 1), and  $\omega$  is the inertia weight factor.

The flowchart of PSO is shown in Fig. 1.

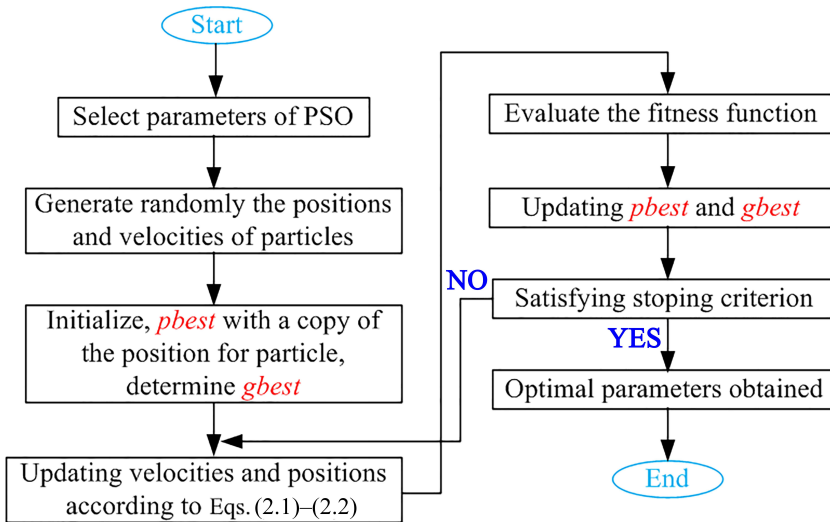


FIG. 1. Flowchart of PSO algorithm.

The main steps of MOPSO are summarized as follows:

- Step 1:* Initialize the population, compute the corresponding objective vectors of particles, and add the non-inferior solutions to the external archive.
- Step 2:* Initialize the local optimum  $pbest$  of particles and the global optimum  $gbest$ .
- Step 3:* Adjust the velocities and positions of the particles by evaluating Eqs. (2.1) and (2.2) to generate a new  $pbest$ .

*Step 4:* Maintain the external archive with the obtained new non-inferior solution, and select *gbest* solution for every particle (the archive determines the selection of global optimum).

*Step 5:* Check whether the maximum iteration is reached, if it is not reached, the program will continue; if it is reached, terminate the computation, and determine the optimal *Pareto* solution set and the *gbest*.

The main difference between PSO and MOPSO is the global optimum and updating of external archive (shown in Fig. 2) that directly determines the *gbest* solution. NDs represent the non-dominated solutions and  $s_1 \sim s_5$  represents a group of solutions.

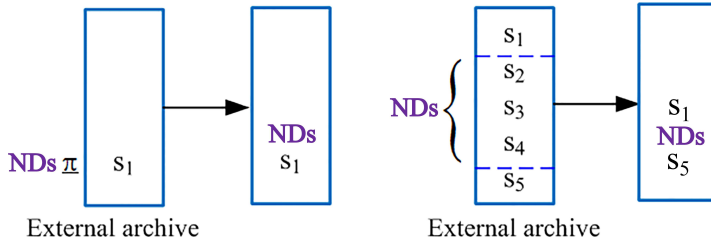


FIG. 2. Updating of external archive.

It is important to point out that direct computation will generate a set of equivalent solutions when traditional multi-objective optimization is performed, and it is difficult to determine which set is the desired one. The *Pareto*-dominating option is the most direct way to solve this problem, namely first by considering all of the non-inferior solutions in the archive, and then generating the *Pareto* frontier by determining a ‘leader’ as shown in Fig. 3. A density measuring technique is commonly used to determine the global optimum, and the nearest neighbor density estimation method [15] based on the nearest neighbor congestion evaluation is adopted here. In this method, a rectangular perimeter consisting of adjacent particles is measured to determine the congestion. This

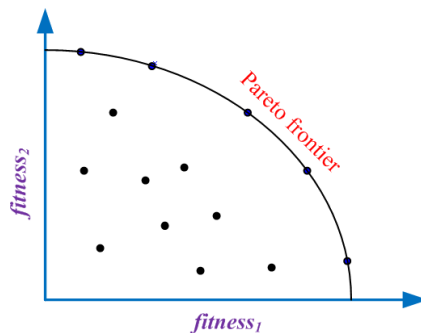


FIG. 3. *Pareto* frontier.

method is schematically depicted in Fig. 4. Certainly, there are other methods such as a kernel density estimation method [16], etc., which determine the global optimum.

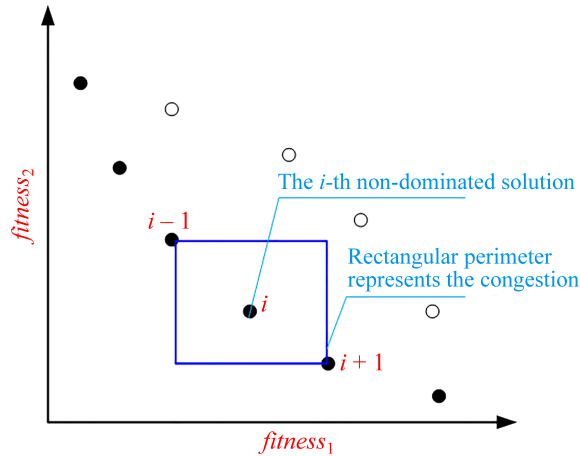


FIG. 4. Schematic diagram of the nearest neighbor density estimation method.

### 3. BRIEF INTRODUCTION TO $H_\infty$ CONTROLLER

A dynamic closed-loop control system is shown in Fig. 5, which indicates the following state space equation:

$$(3.1) \quad \begin{cases} \dot{z}(t) = \mathbf{A}z(t) + \mathbf{b}_1F(t) + \mathbf{b}_2U(t), \\ Y(t) = \mathbf{C}_1z(t) + \mathbf{d}_{11}F(t) + \mathbf{d}_{12}U(t), \\ y(t) = \mathbf{C}_2z(t) + \mathbf{d}_{21}F(t) + \mathbf{d}_{22}U(t), \end{cases}$$

where  $z(t)$  is the state variable,  $y(t)$  is the observation output,  $Y(t)$  is the control output,  $U(t)$  is the control input (namely, this is the generated force of actuator in active vibration control), and  $F(t)$  is the vibration input. Active control with  $H_\infty$  criterion is implemented to design a feedback controller that can make the closed-loop system stable and promote the  $\infty$ -norm of the transfer function  $\|T_{YF}\|_\infty$  minimum.

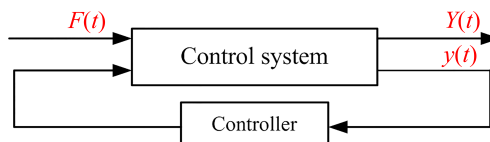


FIG. 5. Dynamic closed-loop control system.

Using the  $\|T_{YF}\|_\infty$  minimum to determine a small value  $\gamma$  which should satisfy the following:

$$(3.2) \quad \|T_{YF}\|_\infty < \gamma.$$

Control input  $U(t)$  in a closed-loop feedback system can be described as

$$(3.3) \quad U(t) = Ky(t),$$

where  $K$  is the gain of feedback controller.

Let us transform Eq. (3.1) to the following state-space equation:

$$(3.4) \quad \begin{bmatrix} \dot{z}(t) \\ Y(t) \\ y(t) \end{bmatrix} = \begin{bmatrix} \mathbf{A} & \mathbf{b}_1 & \mathbf{b}_2 \\ \mathbf{C}_1 & \mathbf{d}_{11} & \mathbf{d}_{12} \\ \mathbf{C}_2 & \mathbf{d}_{21} & \mathbf{d}_{22} \end{bmatrix} \begin{bmatrix} z(t) \\ F(t) \\ U(t) \end{bmatrix}.$$

Then the control input  $U(t)$  can be rewritten as

$$(3.5) \quad U(t) = K(\mathbf{I} - \mathbf{d}_{22}K)^{-1}[\mathbf{C}_2z(t) + \mathbf{d}_{21}F(t)],$$

where  $\mathbf{I}$  is the unit diagonal matrix.

By substituting Eq. (3.5) to Eq. (3.1) the following equation can be obtained:

$$(3.6) \quad \begin{bmatrix} \dot{z}(t) \\ Y(t) \end{bmatrix} = \begin{bmatrix} \mathbf{A}_{cl} & \mathbf{B}_{cl} \\ \mathbf{C}_{cl} & \mathbf{D}_{cl} \end{bmatrix} \begin{bmatrix} z(t) \\ F(t) \end{bmatrix},$$

where

$$\begin{aligned} \mathbf{A}_{cl} &= \mathbf{A} + \mathbf{b}_2K(\mathbf{I} - \mathbf{d}_{22}K)^{-1}\mathbf{C}_2, & \mathbf{B}_{cl} &= \mathbf{b}_1 + \mathbf{b}_2K(\mathbf{I} - \mathbf{d}_{22}K)^{-1}\mathbf{d}_{21}, \\ \mathbf{C}_{cl} &= \mathbf{C}_1 + \mathbf{d}_{12}K(\mathbf{I} - \mathbf{d}_{22}K)^{-1}\mathbf{C}_2, & \mathbf{D}_{cl} &= \mathbf{d}_{11} + \mathbf{d}_{12}K(\mathbf{I} - \mathbf{d}_{22}K)^{-1}\mathbf{d}_{21}. \end{aligned}$$

## 4. ACTIVE VIBRATION CONTROL WITH MULTI-OBJECTIVE CONTROL OUTPUT

### 4.1. Machinery equipment

Let us consider the vibration control model of typical machinery equipment shown in Fig. 6.

In Fig. 6,  $m_1, k_1, c_1$  are respectively the mass, stiffness and damping of foundation or supported structure,  $k_2, c_2$  are respectively the stiffness and damping of isolation system,  $m_2$  is the mass of machinery equipment,  $F_a(t)$  is the active control force generated by actuator, and  $F(t)$  is the disturbance generated by the machinery equipment. The motion equations can be written as

$$(4.1) \quad \begin{cases} m_1\ddot{x}_1 + k_1x_1 + c_1\dot{x}_1 - c_2(\dot{x}_2 - \dot{x}_1) - k_2(x_2 - x_1) = F_a(t), \\ m_2\ddot{x}_2 + c_2(\dot{x}_2 - \dot{x}_1) + k_2(x_2 - x_1) = F(t) - F_a(t). \end{cases}$$

a)



b)

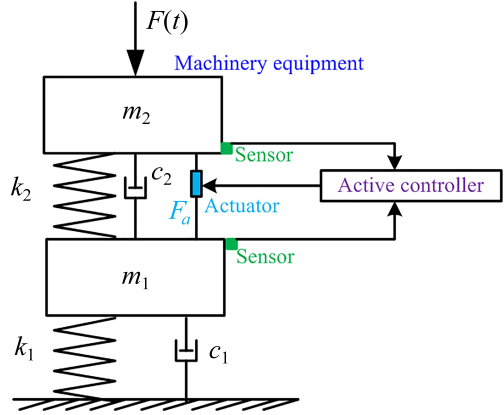


FIG. 6. Active vibration control for machinery equipment: a) machinery equipment, b) model description.

Let us suppose the state variables are  $x_1 = z_1, x_2 = z_2, \dot{x}_1 = z_3, \dot{x}_2 = z_4$ ,  $\mathbf{z} = [z_1, z_2, z_3, z_4]^T$ , then Eq. (4.1) can be rewritten in the state-space form:

$$(4.2) \quad \begin{cases} \dot{z}(t) = \mathbf{A}z(t) + \mathbf{b}_1F(t) + \mathbf{b}_2F_a(t), \\ Y(t) = \mathbf{C}_1z(t) + \mathbf{d}_{11}F(t) + \mathbf{d}_{12}F_a(t), \\ y(t) = \mathbf{C}_2z(t) + \mathbf{d}_{21}F(t) + \mathbf{d}_{22}F_a(t), \end{cases}$$

where

$$\mathbf{A} = \begin{bmatrix} 0 & 0 & 1 & 0 \\ 0 & 0 & 0 & 1 \\ -\frac{k_1 + k_2}{m_1} & \frac{k_2}{m_1} & -\frac{c_1 + c_2}{m_1} & \frac{c_2}{m_1} \\ \frac{k_2}{m_2} & -\frac{k_2}{m_2} & \frac{c_2}{m_2} & -\frac{c_2}{m_2} \end{bmatrix},$$

$$\mathbf{b}_1 = \begin{bmatrix} 0 \\ 0 \\ 0 \\ \frac{1}{m_2} \end{bmatrix}, \quad \mathbf{b}_2 = \begin{bmatrix} 0 \\ 0 \\ \frac{1}{m_1} \\ -\frac{1}{m_2} \end{bmatrix},$$

$$\mathbf{C}_1 = [k_1 \ 0 \ c_1 \ 0], \quad \mathbf{d}_{11} = [0], \quad \mathbf{d}_{12} = [0],$$

$$\mathbf{C}_2 = \begin{bmatrix} 1 & 0 & 0 & 0 \\ 0 & 1 & 0 & 0 \\ 0 & 0 & 1 & 0 \\ 0 & 0 & 0 & 1 \end{bmatrix}, \quad \mathbf{d}_{21} = \begin{bmatrix} 0 \\ 0 \\ 0 \\ 0 \end{bmatrix}, \quad \mathbf{d}_{22} = \begin{bmatrix} 0 \\ 0 \\ 0 \\ 0 \end{bmatrix}.$$

First, the observation output is defined as  $y(t) = [x_1, x_2, \dot{x}_1, \dot{x}_2]^T$ , and the single-objective control output is defined as  $Y(t) = \{k_1 x_1 + c_1 \dot{x}_1\}$ . Next, the multi-objective control output is defined as two indexes, the first one is the force transmitted from the equipment to the foundation:  $Y_1(t) = \{k_1 x_1 + c_1 \dot{x}_1\}$ , and the other one is the velocity of equipment, which implies the vibrating level:  $Y_2(t) = \{\dot{x}_2\}$ . In the active control with the multi-objective control output, the two indexes are expected to be optimized simultaneously, and, then, the state-space equation should be rewritten as

$$(4.3) \quad \begin{cases} \dot{z}(t) = \mathbf{A}z(t) + \mathbf{b}_1 F(t) + \mathbf{b}_2 F_a(t), \\ Y_1(t) = \mathbf{C}_{1,1}z(t) + \mathbf{d}_{1,11}F(t) + \mathbf{d}_{1,12}F_a(t), \\ Y_2(t) = \mathbf{C}_{2,1}z(t) + \mathbf{d}_{2,11}F(t) + \mathbf{d}_{2,12}F_a(t), \\ y(t) = \mathbf{C}_2z(t) + \mathbf{d}_{21}F(t) + \mathbf{d}_{22}F_a(t), \end{cases}$$

where  $\mathbf{A}$ ,  $\mathbf{b}_1$ ,  $\mathbf{b}_2$ ,  $\mathbf{C}_2$ ,  $\mathbf{d}_{21}$  and  $\mathbf{d}_{22}$  are the same as in Eq. (4.2), and  $\mathbf{C}_{1,1} = [k_1 \ 0 \ c_1 \ 0]$ ,  $\mathbf{d}_{1,11} = [0]$ ,  $\mathbf{d}_{1,12} = [0]$ ;  $\mathbf{C}_{2,1} = [0 \ 0 \ 0 \ 1]$ ,  $\mathbf{d}_{2,11} = [0]$ ,  $\mathbf{d}_{2,12} = [0]$ .

In the active control using  $H_\infty$  criterion, a feedback controller can be defined as  $K = [K_1 \ K_2 \ K_3 \ K_4]$ ; furthermore, the following conditions must be satisfied:

- (1) The closed-loop active control must be stable.
- (2) The  $\infty$ -norm of transfer function  $T_{YF}(s, K)$  must satisfy  $\|T_{YF}(s, K)\|_\infty < \gamma$ ,  $\gamma$  is a positive number, where  $s = j\omega_{\text{ref}}$  is the complex frequency, and  $\omega_{\text{ref}}$  is the vibrating frequency.

By combining the PSO and  $H_\infty$  active control, a PSO based  $H_\infty$  active control strategy is adopted here [12], and the fitness function can be defined as

$$(4.4) \quad \|T_{YF}(s, K)\|_\infty.$$

By combining the MOPSO and  $H_\infty$  active control, a MOPSO based active control with a multi-objective control output is proposed here, and the fitness functions are defined as

$$(4.5) \quad \begin{cases} \text{fitness}_1 = \|T_{Y_1 F}(s, K)\|_\infty, \\ \text{fitness}_2 = \|T_{Y_2 F}(s, K)\|_\infty. \end{cases}$$

In view of the PSO based  $H_\infty$  active control studied in [12], a schematic diagram of the proposed active control with multi-objective control output is depicted in Fig. 7.

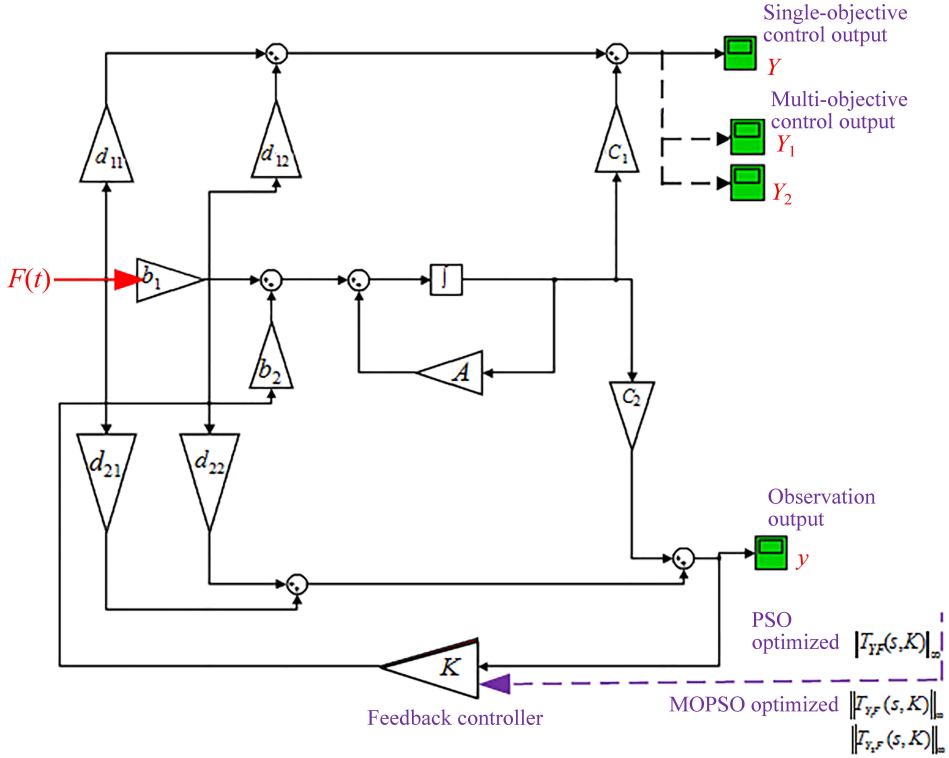


FIG. 7. MOPSO based active control with multi-objective control output.

#### 4.2. Sensitive equipment

Let us now consider the vibration control model of typical sensitive equipment shown in Fig. 8.

In Fig. 8,  $m_1$ ,  $k_1$ ,  $c_1$  are respectively the mass, stiffness and damping of foundation or supported structure,  $k_2$ ,  $c_2$  are respectively the stiffness and damping of isolation system,  $m_2$  is the mass of sensitive equipment,  $F_a(t)$  is the active control force generated by actuator, and  $F(t)$  is the disturbance transmitted from the surrounding environment to the supported structure. The motion equations can be written as

$$(4.6) \quad \begin{cases} m_1 \ddot{x}_1 + k_1 x_1 + c_1 \dot{x}_1 - c_2 (\dot{x}_2 - \dot{x}_1) - k_2 (x_2 - x_1) = F(t) - F_a(t), \\ m_2 \ddot{x}_2 + c_2 (\dot{x}_2 - \dot{x}_1) + k_2 (x_2 - x_1) = F_a(t). \end{cases}$$

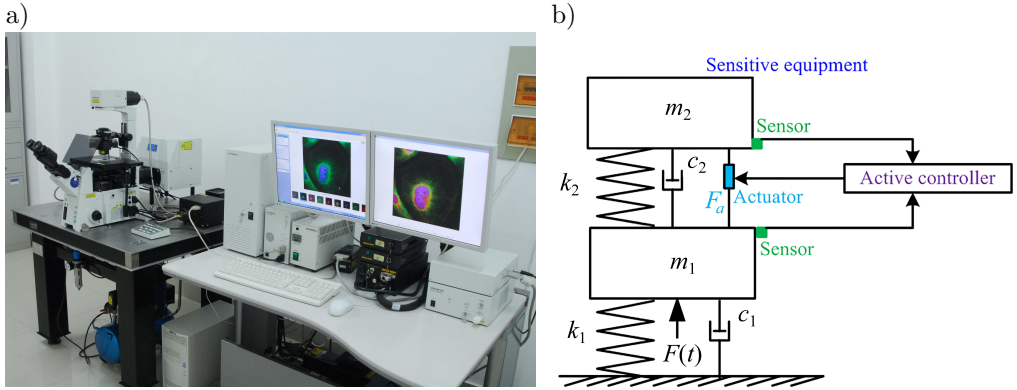


FIG. 8. Active vibration control for sensitive equipment: a) sensitive equipment, b) model description.

Let us suppose the state variables are:  $x_1 = z_1, x_2 = z_2, \dot{x}_1 = z_3, \dot{x}_2 = z_4$ ,  $\mathbf{z} = [z_1, z_2, z_3, z_4]^T$ , then Eq. (4.6) can be rewritten in the state-space form:

$$(4.7) \quad \begin{cases} \dot{\mathbf{z}}(t) = \mathbf{A}\mathbf{z}(t) + \mathbf{b}_1F(t) + \mathbf{b}_2F_a(t), \\ Y(t) = \mathbf{C}_1\mathbf{z}(t) + \mathbf{d}_{11}F(t) + \mathbf{d}_{12}F_a(t), \\ y(t) = \mathbf{C}_2\mathbf{z}(t) + \mathbf{d}_{21}F(t) + \mathbf{d}_{22}F_a(t), \end{cases}$$

where

$$\mathbf{A} = \begin{bmatrix} 0 & 0 & 1 & 0 \\ 0 & 0 & 0 & 1 \\ -\frac{k_1 + k_2}{m_1} & \frac{k_2}{m_1} & -\frac{c_1 + c_2}{m_1} & \frac{c_2}{m_1} \\ \frac{k_2}{m_2} & -\frac{k_2}{m_2} & \frac{c_2}{m_2} & -\frac{c_2}{m_2} \end{bmatrix},$$

$$\mathbf{b}_1 = \begin{bmatrix} 0 \\ 0 \\ \frac{1}{m_1} \\ 0 \end{bmatrix}, \quad \mathbf{b}_2 = \begin{bmatrix} 0 \\ 0 \\ -\frac{1}{m_1} \\ \frac{1}{m_2} \end{bmatrix},$$

$$\mathbf{C}_1 = [0 \ 0 \ 0 \ 1], \quad \mathbf{d}_{11} = [0], \quad \mathbf{d}_{12} = [0],$$

$$\mathbf{C}_2 = \begin{bmatrix} 1 & 0 & 0 & 0 \\ 0 & 1 & 0 & 0 \\ 0 & 0 & 1 & 0 \\ 0 & 0 & 0 & 1 \end{bmatrix}, \quad \mathbf{d}_{21} = \begin{bmatrix} 0 \\ 0 \\ 0 \\ 0 \end{bmatrix}, \quad \mathbf{d}_{22} = \begin{bmatrix} 0 \\ 0 \\ 0 \\ 0 \end{bmatrix}.$$

First, the observation output for sensitive isolation system is also defined as  $y(t) = [x_1, x_2, \dot{x}_1, \dot{x}_2]^T$ , and the single-objective control output is defined as  $Y(t) = \{\dot{x}_2\}$ . For comparison, the multi-objective control output is defined as two indexes, the first one is the vibrating velocity of sensitive equipment:  $Y(t) = \{\dot{x}_2\}$ , and the other one is the deformation of isolators, which is the relative displacement of equipment and supported structure:  $Y_2(t) = \{x_2 - x_1\}$ . In the active control with multi-objective control output, the two control objectives are expected to be optimized simultaneously, and, then, the state space equation could be rewritten in the same form as Eq. (4.3), but the coefficient matrices should be revised as  $\mathbf{C}_{1,1} = [0 \ 0 \ 0 \ 1]$ ,  $\mathbf{d}_{1,11} = [0]$ ,  $\mathbf{d}_{1,12} = [0]$ ;  $\mathbf{C}_{2,1} = [-1 \ 1 \ 0 \ 0]$ ,  $\mathbf{d}_{2,11} = [0]$ ,  $\mathbf{d}_{2,12} = [0]$ ; and  $\mathbf{A}$ ,  $\mathbf{b}_1$ ,  $\mathbf{b}_2$ ,  $\mathbf{C}_2$ ,  $\mathbf{d}_{21}$  and  $\mathbf{d}_{22}$  are the same as in Eq. (4.7).

In the active control using  $H_\infty$  criterion, a feedback controller with the gain vector  $\mathbf{K} = [K_1 \ K_2 \ K_3 \ K_4]$  is also carried out, and the constrained conditions must be satisfied. First, a PSO based  $H_\infty$  active control is performed to give a single-objective output, and the fitness function is defined the same as in Eq. (4.4). Next, a MOPSO based  $H_\infty$  active control is also proposed to give a multi-objective control output, and the fitness functions are defined the same as in Eq. (4.5). Furthermore, the computational diagram is presented in Fig. 7.

## 5. CASE STUDIES

### 5.1. Machinery equipment

Parameters of the vibration isolation system for machinery equipment are  $m_1 = 1200$  kg,  $m_2 = 600$  kg,  $k_1 = 1 \cdot 10^6$  N/m,  $k_2 = 1.5 \cdot 10^4$  N/m,  $c_1 = 1.6 \cdot 10^4$  N·m/s, and  $c_2 = 1 \times 10^3$  N·m/s. The amplitude of vibrating excitation is 1000 N, and the frequency is 2.6 Hz. Parameters of PSO show that the population size of particles = 100, maximum iteration number = 200,  $c_1 = 2$ ,  $c_2 = 1$ , and  $\omega = 0.99^t$  ( $t$  is the iterative number). Constrained condition for optimizing the feedback gain is assumed arbitrarily as

$$\|K\|_\infty \leq 5 \cdot 10^2.$$

The fitness convergence of this single-objective optimization is shown in Fig. 9, and the obtained *gbest* solution is

$$K = [1.913 \ -4.983 \ 1.974 \ -5.000] \cdot 10^2.$$

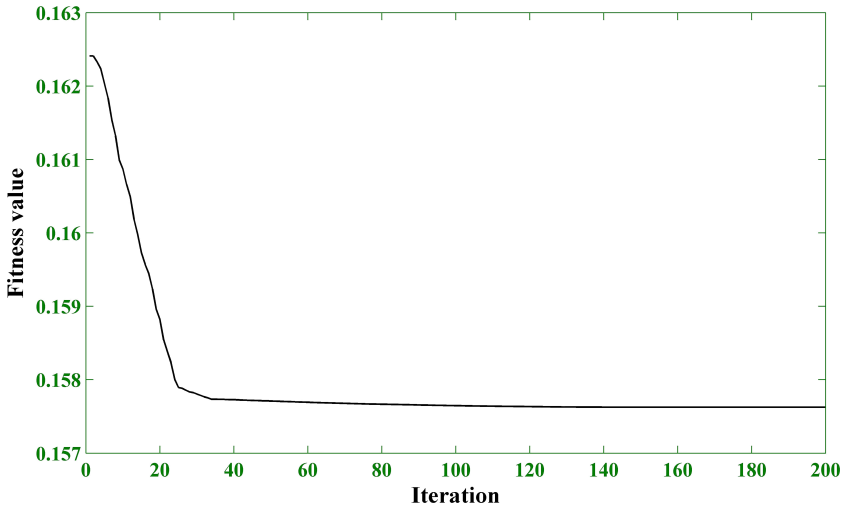


FIG. 9. Fitness convergence of PSO based  $H_\infty$  active control for machinery equipment.

Parameters configuration of MOPSO algorithm is assumed to be the same as in PSO and the *Pareto* frontier of the multi-objective optimization shown in Fig. 10, and the obtained *gbest* solution is

$$K = [ -0.0738 \quad -4.998 \quad 5.000 \quad -1.301 ] \cdot 10^2.$$

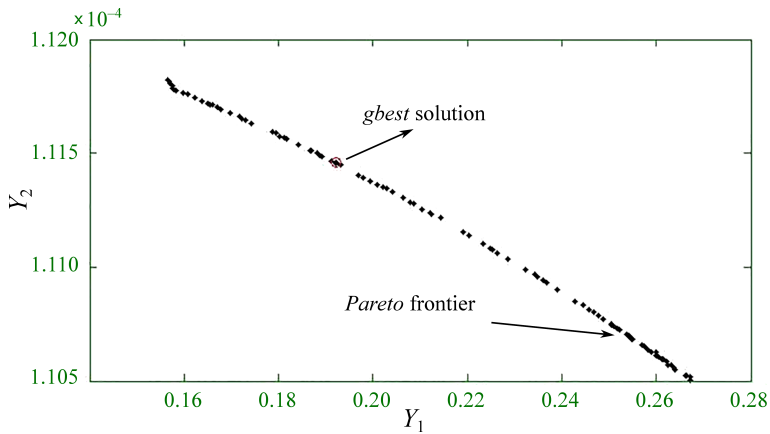


FIG. 10. *Pareto* frontier of MOPSO based  $H_\infty$  active control for machinery equipment.

Based on the optimal feedback controller (*gbest* solution) obtained by the PSO and MOPSO optimized  $H_\infty$  criterion, the force transmitted from the machinery equipment to the foundation and the vibrating velocity of equipment are shown in Fig. 11.

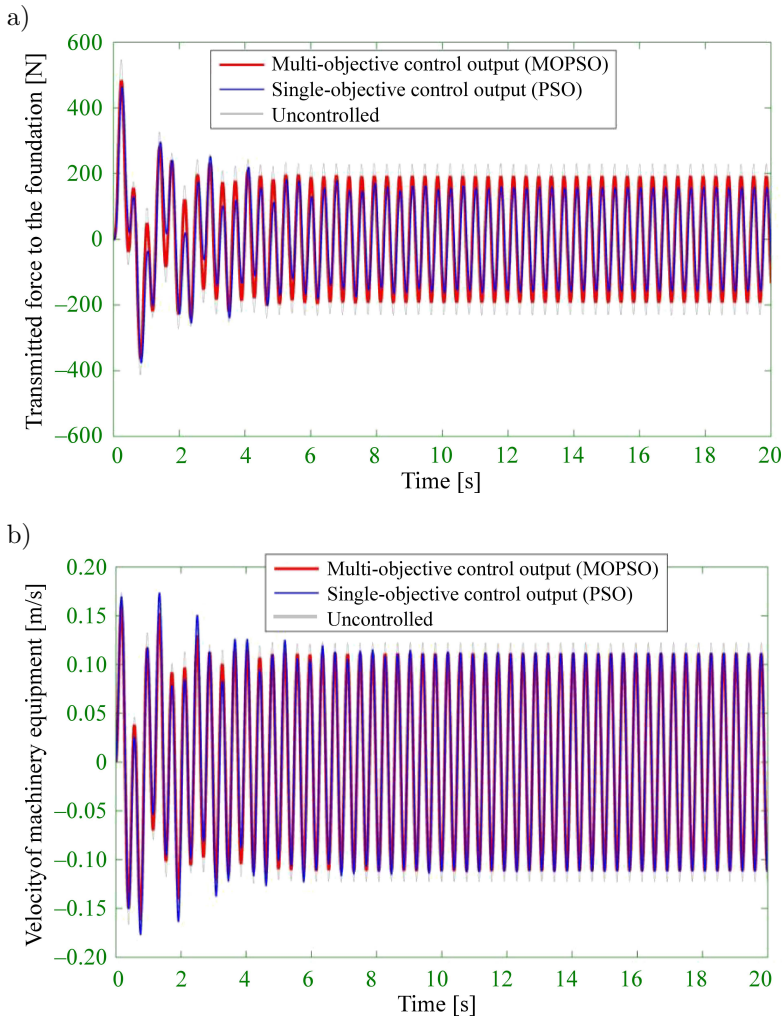


FIG. 11. Comparison of responses of two active controls (machinery equipment): a) force transmitted from the machinery equipment to the foundation, b) vibrating velocity of machinery equipment.

As it can be seen in this figure, the transmitted force under  $\text{PSO-}H_\infty$  condition is indeed better than in the case of multi-objective control output and uncontrolled conditions, however, the control velocity of equipment under  $\text{PSO-}H_\infty$  is bad and it is even worse than under the uncontrolled condition. This latter phenomenon implies that  $\text{PSO-}H_\infty$  has virtually sacrificed the vibrating velocity of equipment for pursuing excellent control of the transmitted force, and this approach is extreme and one-sided. Meanwhile, the two indexes of multi-objective output have been implemented as a balance between the two, and the

active control with multi-objective control output reflects an important role in practice. The comparison of peak responses is listed in Table 1.

**Table 1.** Comparison of peak responses (machinery equipment).

Working conditions	Force transmitted to the foundation	Vibrating velocity of machinery equipment
Multi-objective control output	484.19	0.161
PSO- $H_\infty$	464.27	0.176
Uncontrolled	548.62	0.173

### 5.2. Sensitive equipment

Parameters of the vibration isolation system for sensitive equipment are assumed to be  $m_1 = 1200$  kg,  $m_2 = 100$  kg,  $k_1 = 1 \cdot 10^6$  N/m,  $k_2 = 1.5 \cdot 10^4$  N/m,  $c_1 = 1.6 \cdot 10^4$  N · m/s and  $c_2 = 1 \cdot 10^3$  N · m/s. The amplitude of vibrating excitation is 1 N, and the frequency is 0.6 Hz. Parameters of PSO and MOPSO are the same as in Subsec. 5.1. Constrained condition for optimizing the feedback gain is assumed arbitrarily as

$$\|K\|_\infty \leq 4 \cdot 10^3.$$

Fitness convergence of this single-objective optimization is shown in Fig. 12, and the obtained *gbest* solution is

$$K = \begin{bmatrix} -3.671 & -3.051 & -0.997 & -2.546 \end{bmatrix} \cdot 10^3.$$

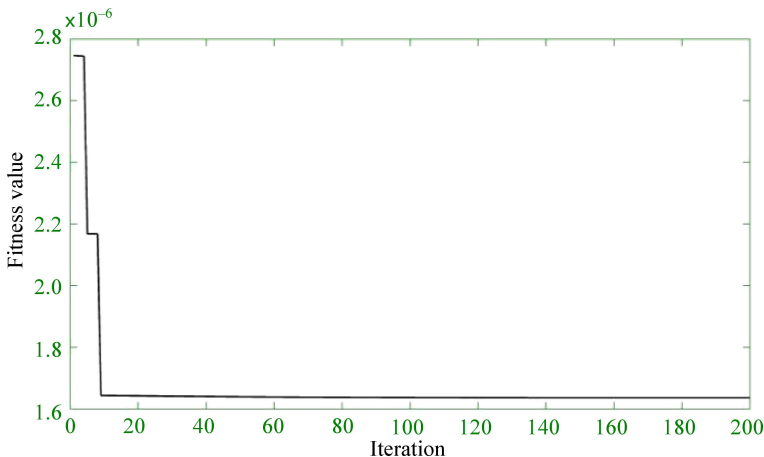


FIG. 12. Fitness convergence of PSO based  $H_\infty$  active control for sensitive equipment.

The *Pareto* frontier of the multi-objective optimization is shown in Fig. 13, and the obtained *gbest* solution is

$$K = [ 0.149 \quad -2.968 \quad 2.498 \quad -2.805 ] \cdot 10^3.$$

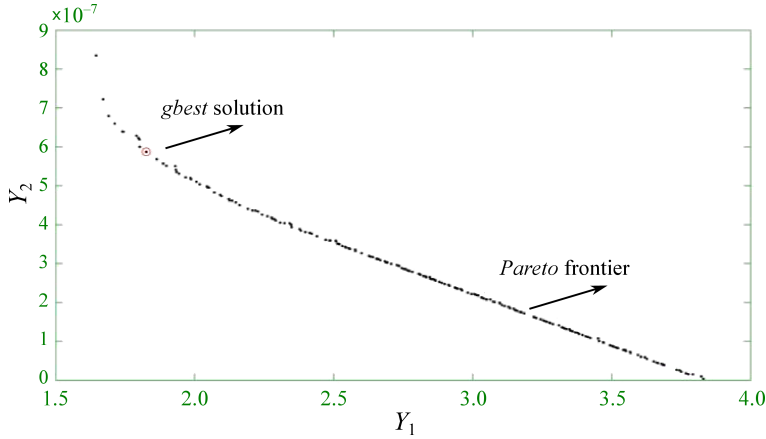


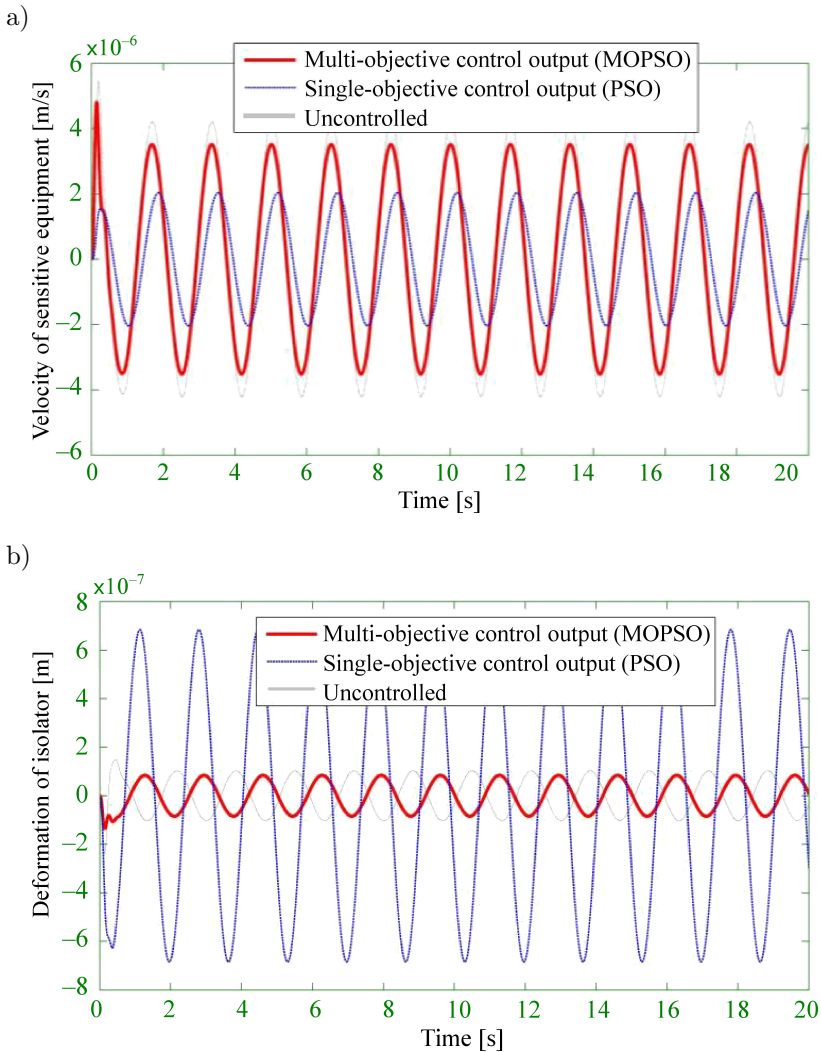
FIG. 13. *Pareto* frontier of MOPSO based  $H_\infty$  active control for sensitive equipment.

Based on the optimal feedback controller (*gbest* solution) obtained by PSO and MOPSO optimized  $H_\infty$  criterion, the vibrating velocity of the sensitive equipment and the deformation of isolator (the relative displacement between the equipment and the supported structure) are shown in Fig. 14.

As it can be seen in Fig. 14, the control velocity of sensitive equipment under PSO- $H_\infty$  condition is better than in the case of the multi-objective control output and uncontrolled conditions; however, the deformation of isolators by PSO- $H_\infty$  is very bad and even it is much worse in the case of the uncontrolled condition, and this phenomenon implies that PSO- $H_\infty$  has potentially sacrificed the deformation of isolators for pursuing an effective control of suppressed velocity of sensitive equipment, and of course this approach is also one-sided. In the meantime, the two indexes of multi-objective control output have again implemented a balance between the two, and multi-objective control output based active control has played a key role. The comparison of peak responses is shown in Table 2.

**Table 2.** Comparison of peak responses (sensitive equipment).

Working conditions	Vibrating velocity of sensitive equipment	Deformation of isolators
Multi-objective control output	$4.831 \cdot 10^{-6}$	$1.372 \cdot 10^{-7}$
PSO- $H_\infty$	$2.037 \cdot 10^{-6}$	$6.848 \cdot 10^{-7}$
Uncontrolled	$5.443 \cdot 10^{-6}$	$2.373 \cdot 10^{-7}$



## 6. CONCLUSIONS

In this study, a novel active control with multi-objective control output by means of artificial intelligence-MOPSO algorithm is proposed, which is aimed at solving a pair of conflicted control indexes, and the traditional active control with single-objective control output is improved; in addition, a PSO based active control is also carried out here for comparison. Numerical results demonstrate that this newly developed strategy is very effective and suitable for the practical

control of machinery and sensitive equipment, and the conflicted indexes can be well balanced as well.

This strategy can serve as inspiration for traditional active vibration control methods, where the multiple indexes, which simultaneously play an important role in the control, can be taken into account at the same time, and, in addition, an extreme and unnecessary pursue of one-sided control output is avoided.

In the future, more than two outputs in the active control will be investigated, and other multi-objective control methods can be presented by improving the artificial intelligence.

#### ACKNOWLEDGMENT

This research was completely supported by National Key Research and Development Program “Research on Vibration Control Technology for Established Industrial Building Structures”, which is sponsored by Ministry of Science and Technology of the P. R. China and the Grant No. is 2016YFC0701302, and it was also launched as a preparation for revising work within ‘Code for design of vibration isolation’ (national code of P. R. China).

We gratefully acknowledge the support of our colleagues in the China National Machinery Industry Corporation (SINOMACH) and in the Technology Research Center of Engineering Vibration Control (EVCC) in China IPPR International Engineering Co., Ltd (IPPR).

#### REFERENCES

1. HARRIS C.M., *Shock and vibration handbook*, pp. 33–50, McGraw-Hill, New York, 1987.
2. BEARD A.M., SCHUBERT D.W., VON FLOTOW A.H., *Practical product implementation of an active/passive vibration isolation system*, SPIE’s 1994 International Symposium on Optics, Imaging, and Instrumentation, International Society for Optics and Photonics, pp. 38–49, 1994.
3. GAWRONSKI W., *Advanced Structural Dynamics and Active Control of Structures*, Springer-Verlag, 2004.
4. PREUMONT A., *Vibration Control of Active Structures*, 3rd ed., Springer, 2011.
5. SPENCER JR. B.F., NAGARAJAIAH S., *State of the Art of Structural Control*, ASCE Journal of Structural Engineering, **129**(7): 845–856, 2003.
6. BLACHOWSKI B., *Model based predictive control of guyed mast vibration*, Journal of Theoretical and Applied Mechanics, **45**: 405–423, 2007.
7. PNEVMATIKOS N., GANTES C., *Control strategy for mitigating the response of structures subjected to earthquake actions*, Engineering Structures, **32**(11): 3616–3628, 2010.
8. KHOT S.M., YELVE N.P., TOMAR R., DESAI S., VITAL S., *Active vibration control of cantilever beam by using PID based output feedback controller*, Journal of Vibration and Control, **18**(3): 366–372, 2012.

9. HUANG W., XU J., ZHU D.Y., LU J.W., LU K.L., HU M.Y., *MOPSO based multi-objective robust  $H_2/H_\infty$  vibration control for typical engineering equipment*, Engineering Transactions, **63**(3): 341–359, 2015.
10. SYMANS M.D, KELLY S.W., *Fuzzy logic control of bridge structures using intelligent semi-active seismic isolation systems*, Earthquake Engineering and Structural Dynamics, **28**(1): 37–60, 1999.
11. EBERHART R.C., KENNEDY J., *A new optimizer using particle swarm theory*, Proceedings of the Sixth International Symposium on Micro Machine and Human Science, pp. 39–42, 1995.
12. FARSHIDIANFAR A., SAGHAFI A., KALAMI S.M., SAGHAFI I., *Active vibration isolation of machinery and sensitive equipment using  $H_\infty$  control criterion and particle swarm optimization method*, Meccanica, **47**(2): 437–453, 2012.
13. Coello Coello C.A., Lechuga M.S., *MOPSO: A proposal for multiple objective particle swarm optimization*, Proceedings of the 2002 Congress on Evolutionary Computation, vol. 2, pp. 1051–1056, 2002, doi: 10.1109/CEC.2002.1004388.
14. SHI Y., EBERHART R., *A modified particle swarm optimizer*, IEEE World Congress on Computational Intelligence, pp. 69–73, 1998.
15. DEB K., PRATAP A., AGARWAL S., MEYARIVAN T., *A fast and elitist multiobjective genetic algorithm: NSGA-II*, IEEE Transactions on Evolutionary Computation, **6**(2): 182–197, 2002.
16. GOLDBERG D.E., RICHARDSON J., *Genetic algorithms with sharing for multimodal function optimization*, Genetic algorithms and their applications: Proceedings of the Second International Conference on Genetic Algorithms, pp. 41–49, 1987.

*Received August 1, 2016; accepted version November 14, 2016.*

---